

Dispersion of graphene in silane coupling agent aqueous solutions

Guo Liping^{1,2,3} Wang Hong¹ Chen Bo⁴ Qian Wenxun⁴

(¹ School of Materials Science and Engineering, Southeast University, Nanjing 211189, China)

(² Jiangsu Key Laboratory of Construction Materials, Southeast University, Nanjing 211189, China)

(³ Collaborative Innovation Centre for Advanced Civil Engineering Materials, Southeast University, Nanjing 211189, China)

(⁴ State Key Laboratory of Hydrology-Water Resources and Hydraulic Engineering,
Nanjing Hydraulic Research Institute, Nanjing 210029, China)

Abstract: In order to reduce the agglomeration of nanographene and improve its dispersibility, six silane coupling agents were used to modify the surface of the nanographene particles. Visual inspection, Fourier-transform infrared spectroscopy, transmission electron microscopy, Raman spectroscopy, and X-ray diffraction were employed to evaluate the dispersion properties of the resulting graphene in an aqueous solution of silane coupling agents. Results show that all six types of silane coupling agents are efficient in promoting the dispersion of graphene in aqueous solutions, and no obvious sedimentation of the graphene dispersion solution is observed after a stationary storage period of 30 d. Taking 3-aminopropyltriethoxysilane (KH-550) as an example, after the graphene is dispersed in the KH-550 aqueous solution, the carboxyl group on the surface of the graphene reacts with the KH-550 amino group to form an amide bond, and KH-550 is successfully grafted onto the graphene surface. Polar functional groups ionize in water, creating an electrostatic repulsion effect, or hydrophilic functional groups form hydrogen bonds with water molecules, which is believed to improve the dispersion stability of graphene. The dispersed graphene is curled and contains many folds. Each fold has about three or four layers, with an interlayer spacing of about 0.65 nm. The dispersed graphene also has a complete lattice and a reduced number of defects. Nanographene disperses well in silane coupling agent aqueous solutions and can, therefore, be used to prepare cement-based composites.

Key words: graphene; silane coupling agent; surface modification; dispersibility

DOI: 10.3969/j.issn.1003-7985.2020.01.009

Graphene is a two-dimensional carbon nanomaterial that is composed of carbon atoms with sp^2 hybridized orbitals, forming a hexagonal honeycomb crystal lat-

tice. It has ultrahigh strength, good electrical conductivity, excellent light transmittance, ultrahigh thermal conductivity, and extremely low resistivity. As a new type of nanomaterial, graphene is widely used in the building materials industry for optimizing the interface transition zone and microstructure of concrete^[1-2], enhancing its durability^[3], reducing its resistance^[4], and improving its mechanics and deformation performance^[5-7]. Moreover, graphene has been reported to add new functions to admixtures^[8-9] as well as many other aspects. However, owing to the small particle size and high surface energy of graphene, the resultant strong van der Waals force between graphene layers facilitates agglomeration and formation of secondary particles, compromising the expected outcomes in terms of surface area, volume, and quantum size effects. Therefore, improving the dispersion performance is the basic premise for the popularization and application of graphene^[10-11]. Surface modification of nanoparticles by coupling agents is a cost-effective and efficient surface treatment method for improving the dispersion of graphene. The surface of the particles is modified by chemical coupling, where ionic or covalent bonds between the two coupled groups are allowed in addition to the interaction of the van der Waals force, hydrogen bond, or coordination bond^[12-13]. Coupling agents such as organoaluminate, titanate, and silane coupling agents are commonly used^[14]. However, the effect of coupling agents on the dispersion of modified nanographene still lacks systematic experimental analysis. In this paper, six types of silane coupling agents were selected to modify the surface of nanographene. Taking 3-aminopropyltriethoxysilane (KH-550) as an example, the dispersion properties of graphene in an aqueous solution of silane coupling agents were systematically studied by visual inspection and microscopic measurements, which provided technical support for the application of graphene in cement-based composites.

1 Materials and Methods

1.1 Materials

Multilayer conductive graphene nanosheets were selected, whose technical specifications are shown in Tab. 1.

Received 2019-10-03, **Revised** 2020-01-07.

Biography: Guo Liping (1979—), female, doctor, associate professor, guoliping691@163.com.

Foundation items: The National Key R & D Program of China (No. 2018YFC0406701), the National Natural Science Foundation of China (No. 51778133, 51739008).

Citation: Guo Liping, Wang Hong, Chen Bo, et al. Dispersion of graphene in silane coupling agent aqueous solutions[J]. Journal of Southeast University (English Edition), 2020, 36(1): 67–72. DOI: 10.3969/j.issn.1003-7985.2020.01.009.

Tab. 1 Technical properties of the nanographene sheets

Specific surface area/($\text{m}^2 \cdot \text{g}^{-1}$)	Particle size(D50)/ μm	Carbon content/%	Oxygen content/%	Sulfur content/%	Conductivity/($\text{S} \cdot \text{m}^{-1}$)
200 \pm 25	7.0 \pm 1.0	<98	<0.5	<0.1	>4 000

The silane coupling agents used are γ -diethylenetriaminopropyl methyl dimethoxysilane (KH-103), KH-550, N-(β -aminoethyl)- γ -aminopropyltriethoxysilane (KH-791), N- β -aminoethyl- γ -aminopropyl methyl dimethoxysilane (KH-602), 3-urea propyl trimethoxysilane (KH-152), and 3-urea propyl triethoxysilane (KH-160). These six coupling agents are stable in alkaline media.

1.2 Graphene dispersion process

1 g of silane coupling agent was dissolved in 100 mL of deionized water. The beaker containing the silane coupling agent solution was then placed on a magnetic stirrer, and 0.1 g of graphene was added while stirring. The magnetic stirring lasted 2 to 3 min. Then, the preliminary dispersion was further dispersed by ultrasonic waves for 1 h (ultrasonic frequency 20 kHz, power 2 kW). A flow-chart of the dispersion process is shown in Fig. 1.

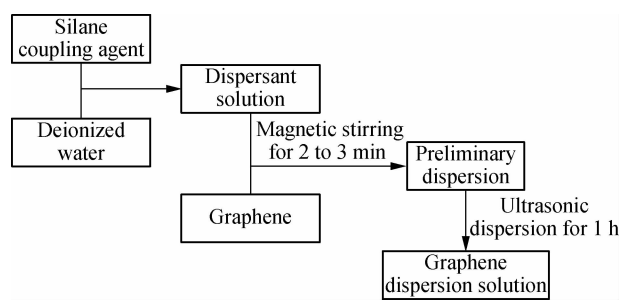


Fig. 1 A flowchart of the graphene dispersion process

1.3 Test method

The surface functional groups of graphene were determined using the Fourier-transform infrared spectroscopy (FT-IR, Nicolet 5700). Small amounts of graphene were mixed with KBr for grinding. Moisture proofing should be paid attention to during grinding. A proper amount of uniformly mixed graphene and KBr was used for tableting, to yield uniform and transparent tablets.

The micromorphology of graphene was observed using the transmission electron microscopy (TEM, G220). The graphene dispersion was diluted 100 times, and a drop of the dispersion solution was taken up on a copper mesh, dried, and tested.

The number of layers and defects in the graphene samples was determined using the laser micro-Raman spectroscopy. Graphene was dispersed in water, and a drop of the aqueous solution was transferred to a 10 \times 10 mm single crystal silicon wafer by a pipette, forming a uniform layer.

The structure of graphene was assessed using a Smart LabX tomographic X-ray diffractometer with Cu $K\alpha$ radi-

ation generated at 30 mA and 40 kV. Samples were scanned from 5° to 80° at 0.02° 2 θ steps integrated at a rate of 2°/min. Samples of different dispersion durations were taken, and the prepared powder samples were placed in a vacuum oven at 60 °C for 24 h prior to the tests. X-ray diffraction (XRD) pattern analysis was performed using the software Jade 5.0.

2 Results and Discussion

2.1 Evaluation of the dispersion effect

The precipitation of the dispersed liquid was observed by visual inspection. The silane coupling agents used were all transparent, colorless liquids, and the stability of the graphene suspension can be judged by observing the uniformity of the solution's color and its stratification. Fig. 2 shows the homogeneity and stratification of the dispersed liquid after different periods of time, such as 10 min, 30 min, 1 d, and 30 d.

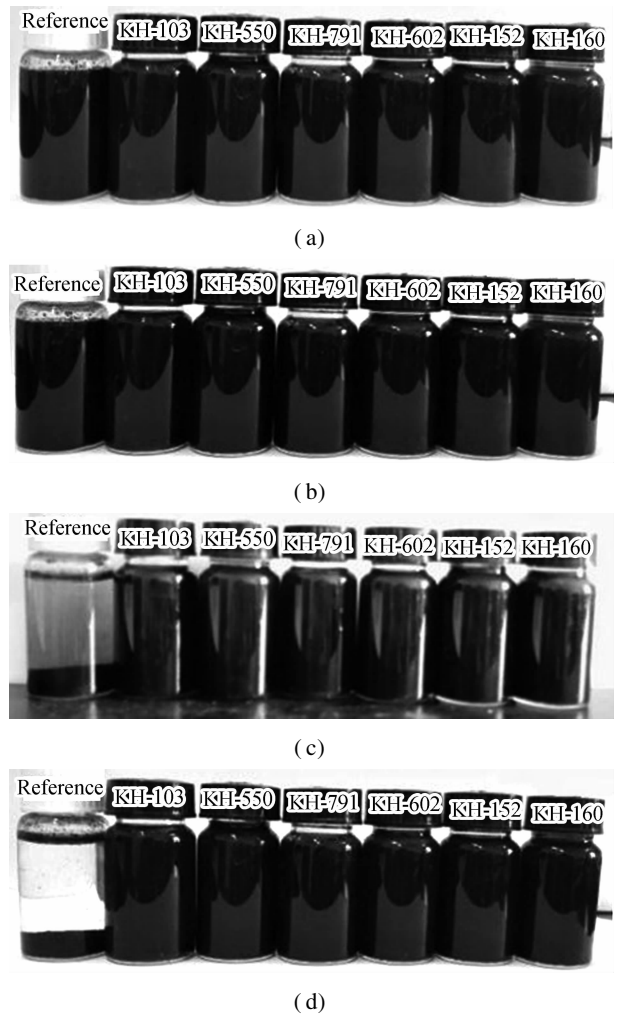


Fig. 2 Pictures of graphene dispersed solutions after different periods of time. (a) 10 min; (b) 30 min; (c) 1 d; (d) 30 d

For the reference group without any dispersant, a small amount of graphene aggregates floated on the surface of the dispersion solution after 10 min, owing to the noninfiltration of the graphene surface. After standing for 30 min, precipitation began to appear in the upper part of the dispersion solution, which gradually became clear. After standing for 24 h, precipitation was almost complete, and the supernatant showed a microsuspension state. At the end of the 30 d, graphene had completely precipitated, and there were no suspended graphene particles in the supernatant, except for a small amount of agglomerated particles attached to the bottle wall.

Graphene showed good dispersion stability in all six silane coupling agents tested. After standing for 30 d, the color of the dispersion remained unchanged, and no obvious precipitation or delamination was observed. The degree of dispersion stability is sufficient to meet the requirements for the preparation of cementitious composites.

2.2 Analysis of the dispersion performance

2.2.1 FT-IR analysis

In the process of ultrasonic dispersion, agglomerated graphene layers are unfolded and graphene materials with fewer layers are formed. During the dispersion process, a large number of functional groups are introduced on the graphene surface. The dispersing agent reacts with the functional groups on the surface of graphene or is absorbed by the graphene's surface. Electrostatic repulsion occurs on the graphene's surface by hydrolysis or ionization so that it can be stably dispersed. The dispersion mechanism of graphene in dispersants is analyzed by taking KH-550 as an example.

In order to compare the changes of the surface functional groups of graphene before and after dispersion, infrared analyses of the original graphene (OG) and graphene modified with KH-550 (MG) were carried out. The results are shown in Fig. 3.

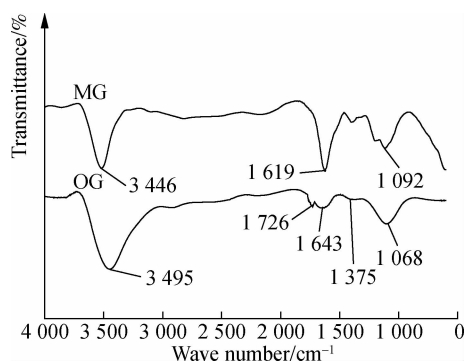
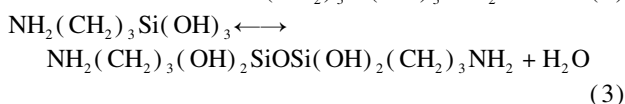
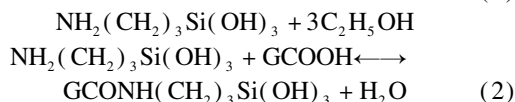
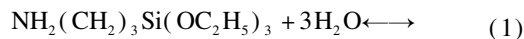


Fig. 3 Graphene FT-IR spectrum

In Fig. 3, OG shows the FT-IR spectrum of graphene without dispersion agent. The peak at 3495 cm⁻¹ corresponds to the stretching vibration peak of —OH in graphene, and the peak at 1726 cm⁻¹ corresponds to the

C=O stretching vibration peak at the edge of the graphene layer. A characteristic vibrational peak is seen at 1643 cm⁻¹; meanwhile, deformation and absorption vibrations are ascribed to the peaks at 1375 and 1068 cm⁻¹, respectively. MG shows the FT-IR spectra of graphene dispersed by KH-550. The bending vibration absorption peak of —CONH— appears at 1619 cm⁻¹, which indicates the formation of amide bonds. This indicates that amide bonds are formed by the chemical reaction between the amino groups in KH-550 and the graphene surface, or carboxyl groups are adsorbed on the graphene's surface. At the same time, the stretching vibration peak of Si—O—Si appears at 1092 cm⁻¹, likely formed by hydrolysis and the condensation of alkoxy groups on the graphene's surface^[15]. In summary, the underlying process can be explained by the reaction of the carboxyl and amino groups on the surface of graphene to form amide bonds after dispersion by KH-550. Thus, KH-550 is successfully grafted onto the surface of graphene. These polar functional groups ionize in water, creating an electrostatic repulsion effect, or alternatively hydrophilic functional groups easily form hydrogen bonds with water molecules, increasing the hydrophilicity of graphene and enabling infiltration and dispersion. The reaction equations involved in the dispersion process are as follows:



2.2.2 TEM analysis

In order to provide a more intuitive illustration of the dispersion effect caused by the silane coupling agents on the graphene samples, TEM images were taken before and after dispersion, and the results are shown in Fig. 4. In Fig. 4(a), a micrograph of the graphene nanosheet that has not been subjected to dispersion treatment reveals a clear agglomeration state, with a thicker middle portion and thinner edges.

A selected area electron diffraction (SAED) image is shown in Fig. 4(b). The SAED patterns of the graphene aggregates are similar to those of graphite, and the crystallinity of the graphene aggregates is good. Figs. 4(c) and (d) show the TEM images of the graphene nanosheets dispersed by KH-550. We observed the formation of a film-like structure with many folds, in a curled state, in line with the expected result from a process driven thermodynamically toward the reduction of the system's Gibbs energy. The layers of the graphene nanosheets cannot be accurately assessed from the TEM images but can

be estimated by edge warping and fold width. Through the analysis of electron diffraction images of a selected area, the dispersed graphene has three to four layers thickness and the lattice structure is complete. Therefore, we conclude that the dispersion method reported here using silane coupling agents yields a stable and uniform graphene aqueous dispersion.

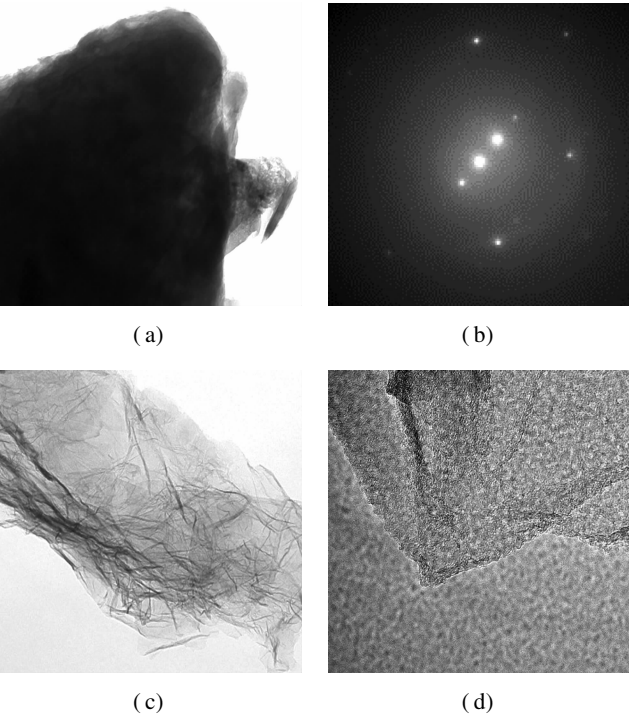


Fig. 4 TEM image and SAED patterns of the graphene and modified graphene samples. (a) Unmodified graphene sample; (b) SAED of the sample shown in (a); (c) TEM of the modified graphene sample; (d) TEM of the modified graphene at a higher magnification

2.2.3 Analysis by Raman spectroscopy

In order to further characterize the layers and the lattice structures of the graphene formed before and after dispersion, Raman spectra were assessed, which are shown in Fig. 5. There are three distinct diffraction peaks in Figs. 5 (a) and (b). The first diffraction peak is the *D*-peak. The sharper the *D*-peak, the more defects the graphene has. The second peak is the *G*-peak, which indicates that the carbon atoms are combined in an sp^2 hybridized manner. The last peak is a *2D*-peak, whose separation tendency indicates that the graphene is multilayered; the larger the ratio of the *2D*-peak intensity to the *G*-peak intensity $R_{2D/G}$, the smaller the number of graphene layers.

A sharp *D*-peak can be seen in Fig. 5 (a), indicating that the graphene has many defects. In addition, the peak separation tendency of the *2D*-peak indicates a multilayered graphene nature, with $R_{2D/G} = 0.082$. In Fig. 5 (b), the *D*-peak is short and relatively flat, indicating that the graphene defects are reduced after dispersion, and $R_{2D/G} = 0.375$ indicates that the number of graphene layers after

dispersion is much smaller than that before dispersion. Before dispersion, the graphene is agglomerated in an unordered manner, so it looks disorganized overall and the overall defects increase; after dispersion, the graphene is arranged in an orderly manner, and the overall defects are much reduced. This is also consistent with the TEM image analysis results.

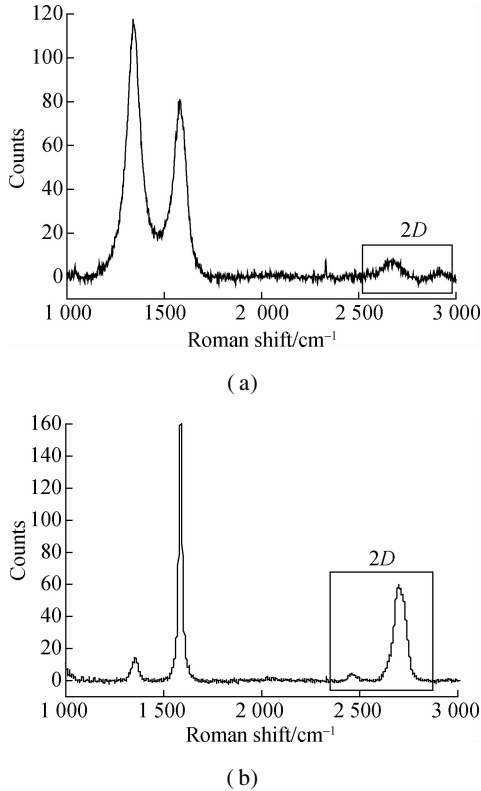


Fig. 5 Raman spectra of unmodified graphene and modified graphene. (a) Unmodified graphene; (b) Modified graphene

2.2.4 XRD analysis

In order to compare the structural changes of graphene before and after modification, the phase structure of OG and MG was characterized using XRD, as shown in Fig. 6. As can be seen from the figure, OG has a high-intensity, narrow diffraction peak at $2\theta = 13.78^\circ$, with a layer spacing of 0.65 nm, as calculated by the Bragg equation.

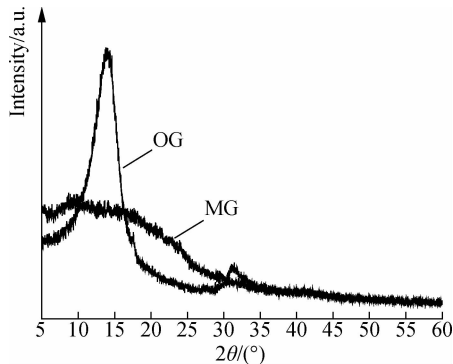


Fig. 6 XRD patterns of OG and MG

Compared with the graphite diffraction peak mentioned in Ref. [16], the diffraction peak shifts by about 13° to the left, and the spacing increases almost twice. After being dispersed by KH-550, the sharp diffraction peak of graphene becomes a broad, subtle peak. This is because the intercalation of KH-550 into graphene increases the interlayer spacing, and the alkoxy group in KH-550 molecules may hydrolyze and condensate with another nearby alkoxy group, which makes the graphene particles join together from different angles, thus forming a disordered structure, resulting in a broad, subtle MG diffraction peak.

3 Conclusions

1) By studying the dispersion of graphene in an aqueous solution containing silane coupling agents, it is found that all the six agents tested here, namely, KH-103, KH-550, KH-791, KH-602, KH-152, and KH-160, are efficient in promoting the dispersion of graphene in aqueous media. Samples are left to stand for 30 d, and no significant sedimentation is observed.

2) Silane coupling agents are adsorbed on the graphene's surface after hydrolysis in aqueous solutions or condense with carboxyl groups so that amino groups can form amide bonds on the surface. These polar functional groups ionize in water; through electrostatic repulsion, or hydrogen bonds formed between the hydrophilic functional groups and water molecules. The hydrophilicity of graphene is increased, enabling infiltration and dispersion.

3) The dispersed graphene is curled and contains a large number of folds. Each fold has about three or four layers, with an interlayer spacing of about 0.65 nm. The dispersed graphene obtained has a complete lattice and a reduced level of defects.

References

- [1] Guo K, Ma H H, Wang Q. Effect of graphene oxide on interfacial transition zone of recycled concrete[J]. *Journal of Architecture and Civil Engineering*, 2018, **35**(5): 217 – 224. (in Chinese)
- [2] Lü S H, Ding H D, Sun T, et al. Effect of naphthalene superplasticizer/graphene oxide composite on microstructure and mechanical properties of hardened cement paste [J]. *Journal of Shaanxi University of Science & Technology (Natural Science Edition)*, 2014, **32**(5): 42 – 47. (in Chinese)
- [3] Yang Y L, Yuan X Y, Shen X, et al. Research on the corrosion resistance of graphene oxide on cement mortar [J]. *Journal of Functional Materials*, 2017, **48**(5): 5144 – 5148. (in Chinese)
- [4] Zhang Y M, Yu L H. Mechano-electric effect of steel fiber and graphene reinforced conductive concrete during flexural process[J]. *Concrete*, 2016(2): 52 – 55, 59. (in Chinese)
- [5] Lei B, Zou J, Rao C H, et al. Experimental study on modification of recycled concrete with graphene oxide[J]. *Journal of Building Structures*, 2016, **37**(S2): 103 – 108. DOI: 10.14006/j.jzjgxb.2016.s2.015. (in Chinese)
- [6] Lü S H, Ma Y J, Qiu C C, et al. Study on reinforcing and toughening of graphene oxide to cement-based composites[J]. *Journal of Functional Materials*, 2013, **44**(15): 2227 – 2231. (in Chinese)
- [7] Li X Y, Korayem A H, Li C Y, et al. Incorporation of graphene oxide and silica fume into cement paste: A study of dispersion and compressive strength[J]. *Construction and Building Materials*, 2016, **123**: 327 – 335. DOI: 10.1016/j.conbuildmat.2016.07.022.
- [8] Gao D G, Ma Y J. Preparation and properties of copolymer of graphene oxide and monomers of polycarboxylate superplasticizer[J]. *Fine Chemicals*, 2015, **32**(1): 103 – 107, 120. DOI: 10.13550/j.jxhg.2015.01.021. (in Chinese)
- [9] Zhao L, Guo X L, Ge C, et al. Mechanical behavior and toughening mechanism of polycarboxylate superplasticizer modified graphene oxide reinforced cement composites [J]. *Composites Part B: Engineering*, 2017, **113**: 308 – 316. DOI: 10.1016/j.compositesb.2017.01.056.
- [10] Li D, Müller M B, Gilje S, et al. Processable aqueous dispersions of graphene nanosheets[J]. *Nature Nanotechnology*, 2008, **3**(2): 101 – 105. DOI: 10.1038/nnano.2007.451.
- [11] Chuah S, Li W G, Chen S J, et al. Investigation on dispersion of graphene oxide in cement composite using different surfactant treatments[J]. *Construction and Building Materials*, 2018, **161**: 519 – 527. DOI: 10.1016/j.conbuildmat.2017.11.154.
- [12] Xu P J, Yan X T, Cong P L, et al. Silane coupling agent grafted graphene oxide and its modification on polybenzoxazine resin [J]. *Composite Interfaces*, 2016, **24**(7): 635 – 648. DOI: 10.1080/09276440.2017.1254989.
- [13] Zhang X Y, Shen H F, Huang H, et al. Novel progress of application and surface-modification technique for nanoparticles materials[J]. *Journal of Materials Engineering*, 2005, **33**(10): 58 – 63. (in Chinese)
- [14] Guo L P, Lei D Y, Chen B, et al. Surface modification and dispersibility evaluation of silica fume[J]. *Surface Technology*, 2018, **47**(7): 146 – 151. DOI: 10.16490/j.cnki.issn.1001-3660.2018.07.020. (in Chinese)
- [15] Fu L L. *Analysis and detection technology of polymer materials*[M]. Beijing: Chemical Industry Press, 2014: 50 – 65.
- [16] Pan Z, He L, Qiu L, et al. Mechanical properties and microstructure of a graphene oxide-cement composite[J]. *Cement and Concrete Composites*, 2015, **58**: 140 – 147. DOI: 10.1016/j.cemconcomp.2015.02.001.

石墨烯在硅烷偶联剂水溶液中的分散性能

郭丽萍^{1,2,3} 王 虹¹ 陈 波⁴ 钱文勋⁴

(¹ 东南大学材料科学与工程学院, 南京 211189)

(² 东南大学江苏省土木工程材料重点实验室, 南京 211189)

(³ 东南大学先进土木工程材料协同创新中心, 南京 211189)

(⁴ 南京水利科学研究院水文水资源与水利工程科学国家重点实验室, 南京 210029)

摘要: 为了降低纳米石墨烯的团聚现象、提高其分散性能, 采用 6 种硅烷偶联剂对纳米石墨烯颗粒进行了表面改性, 并采用目测法、傅里叶红外光谱、透射电镜、拉曼光谱和 X 射线衍射等方法, 对石墨烯在硅烷偶联剂水溶液中的分散性能进行了评价. 结果表明: 6 种硅烷偶联剂对促进石墨烯在水溶液中分散有较好的效果, 石墨烯分散液静置 30 d 未见明显沉降; 以 3-氨丙基三乙氧基硅烷(KH-550)为例, 石墨烯在 KH-550 水溶液种分散后, 石墨烯表面的羧基和 KH-550 的氨基反应生成酰胺键, KH-550 成功接枝在石墨烯表面, 极性官能团在水中电离形成静电排斥效应, 或亲水官能团与水分子形成氢键, 提高了石墨烯的分散稳定性; 分散后的石墨烯呈卷曲状态, 含大量褶皱, 厚度大致 3~4 层厚, 层间距约为 0.65 nm, 晶格完整, 缺陷减少. 纳米石墨烯在在硅烷偶联剂水溶液中的分散性较好, 可用于制备水泥基复合材料.

关键词: 石墨烯; 硅烷偶联剂; 表面改性; 分散性

中图分类号: TU528